JBC RESEARCH ARTICLE

Domains required for the interaction of the central negative element FRQ with its transcriptional activator WCC within the core circadian clock of *Neurospora*

Received for publication, February 25, 2023, and in revised form, May 4, 2023 Published, Papers in Press, May 21, 2023,
https://doi.org/10.1016/j.jbc.2023.104850

Bin Wang (王斌)* and **Jay C. Dunlap**

From the Department of Molecular and Systems Biology, Geisel School of Medicine at Dartmouth, Hanover, New Hampshire, USA

Reviewed by members of the JBC Editorial Board. Edited by Ursula Jakob

In the negative feedback loop composing the *Neurospora* circadian clock, the core element, FREQUENCY (FRQ), binds with FRQ-interacting RNA helicase (FRH) and casein kinase 1 to form the FRQ–FRH complex (FFC) which represses its own expression by interacting with and promoting phosphorylation of its transcriptional activators White Collar-1 (WC-1) and WC-2 (together forming the White Collar complex, WCC). Physical interaction between FFC and WCC is a prerequisite for the repressive phosphorylations, and although the motif on WCC needed for this interaction is known, the reciprocal recognition motif(s) on FRQ remains poorly defined. To address this, we assessed FFC–WCC in a series of *frq* segmental-deletion mutants, confirming that multiple dispersed regions on FRQ are necessary for its interaction with WCC. Biochemical analysis shows that interaction between FFC and WCC but not within FFC or WCC can be disrupted by high salt, suggesting that electrostatic forces drive the association of the two complexes. As a basic sequence on WC-1 was previously identified as a key motif for WCC–FFC assembly, our mutagenetic analysis targeted negatively charged residues of FRQ, leading to identification of three Asp/Glu clusters in FRQ that are indispensable for FFC–WCC formation. Surprisingly, in several *frq* Asp/Glu-to-Ala mutants that vastly diminish FFC–WCC interaction, the core clock still oscillates robustly with an essentially wildtype period, indicating that the interaction between the positive and negative elements in the feedback loop is required for the operation of the circadian clock but is not a determinant of the period length.

Circadian rhythms control a wide range of cellular and behavioral processes in most eukaryotes and certain prokaryotes (1, 2), facilitating adaptation of life to constant environmental changes; disruption of circadian rhythms has been implicated in various diseases in humans (3). At the molecular level, circadian clocks rely mainly on interlocked positive and negative arms, and in circadian cycles, the latter gradually repress their own expression through inactivating the former on a timescale of hours. In the clock of *Neurospora crassa*, a circadian model organism used for decades, the White Collar complex (WCC) derived from all cellular White Collar-1 (WC-1) and a fraction of WC-2 drives transcription of the central pacemaker gene, *frequency* (*frq*), through binding to either of two DNA elements in the *frq* promoter under contrasting illumination conditions: either the *Clock box* (*C-box*) in the dark or the *proximal light-response element* upon light exposure or in constant light (4–6). FREQUENCY (FRQ), encoded by the *frq* gene, associates with FRH (FRQ-interacting RNA helicase) (7–9) and CK1 (casein kinase 1) (10) to create the FFC (FRQ–FRH complex), repressing WCC transcriptional activity by promoting its phosphorylation at a group of residues: S971, S988, S990, S992, S994, and S995 of WC-1 as well as S331, T339, S341, S433, and T435 of WC-2 (10–12) and thereby terminating its own expression to conclude a circadian cycle.

An orthologous feedback loop is found in mammalian cells, with CLOCK and BMAL1 forming a heterodimer that plays the role of WCC, driving expression of PERIODs (PERs) and CRYPTOCHROMEs (CRYs) which form a negative element complex with CK1, analogous to the FFC, that inactivates CLOCK/BMAL1 by phosphorylation at key residues (13, 14). As is the case in *Neurospora*, while much is becoming known about the means through which repression is achieved (14–18), relatively little is known about the structural determinants on PERs/CRYs or CLOCK/BMAL1 that determine their interactions.

In *Neurospora*, WCC acts as a responsive hub coordinating the circadian clock that is obligate in constant darkness and light signaling (19). In consonance with its dual role as a light sensor and a transcription factor for *frq* in the clock, WC-1 bears a light-, oxygen-, and voltage-sensing domain, a transactivation domain, two motifs required for DNA binding—the zinc finger (ZnF) and its nearby DBD (defective in DNA binding) motif, and two Per-Arnt-Sim (PAS) domains for WC-2 interaction (20, 21); WC-2, an accessory of WC-1, contains a PAS and a ZnF DNA-binding domain (20). The DBD motif (KKKRKRRK) on WC-1 has been discovered to be indispensable for WCC to bind the *C box* and to drive *frq* transcription in the dark as well as for interacting with FRQ/FRH (21).

FRQ functions mainly as an organizing platform for recruiting and scaffolding the circadian negative elements FRH and CK1 in forming the FRQ–FRH–CK1 complex which controls the pace of the clock (7, 22). Self-interaction among

* For correspondence: Bin Wang, Bin.Wang@Dartmouth.edu.

FRQ molecules occurs *via* their coiled-coil domains and disruption of the coiled-coil results in arrhythmicity (23). The nuclear localization signal of FRQ is necessary for its circadian function in WCC repression (24). FRQ interacts with CK1 through two domains: FRQ-CK-1a interaction domain 1 (25) and FRQ-CK-1a interaction domain 2 (10) and with FRH *via* the FRQ–FRH interaction domain (7, 26). FRQ also contains two PEST-like elements: PEST-1 and PEST-2, both of which undergo CK-1a- and CK-1b-mediated progressive phosphorylations, and elimination of PEST-1 results in arrhythmic conidiation, reflecting an impaired clock (27). Intramolecular interplay between the N and C termini of FRQ has been shown to be key for the clock operation (25).

Multisite phosphorylation has been investigated extensively as a major mechanism for fine-tuning circadian activities of both FRQ (10, 28–30) and its transcriptional factor WCC (10–12, 31). Many phosphorylation isoforms of FRQ have been reproducibly seen in Western blotting from cultures grown in the light (32). As the initial step in feedback-loop execution, negative elements need to interact physically with the positive factors in order to promote posttranslational modifications to the latter and thereby bring about timely but gradual repression. While prior work on the *Neurospora* clock has focused on phosphorylation and transcription-centered mechanisms controlling the clock, it remains largely unknown how molecular contacts between the positive and negative element complexes are accomplished, though this step is plainly required for subsequent negative feedback inhibition. We previously uncovered a motif on WC-1 composed of eight consecutive highly basic residues required for interaction with FRQ (21), raising the corresponding question of which regions and residues of FRQ are reciprocally involved in the establishment of FFC–WCC. To tackle this puzzle, here we have characterized key regions of FRQ essential for the WCC–FFC interaction and also the operation of the core circadian oscillator. As biochemical data hinted that FFC and WCC may contact *via* electrostatic charges, we focused on negatively charged residues falling in the important regions of FRQ that determine WCC interaction. To this end, mutagenetic analyses revealed three clusters of FRQ residues that contribute to WCC association. Interestingly, however, the core clock still runs normally in certain *frq* mutants with an extremely low level of FFC–WCC, revealing that while interaction between the positive and negative elements is required for the circadian feedback mechanism, it is not a reliable measurement for period length.

Results

A frq *deletion series identifies regions required for the* Neurospora *clock*

Three distinct regions on FRQ have been implicated in WCC interaction: amino acids 107 to 310, 435 to 558, and 631 to 905 (26). The loss of FRQ–WCC interaction in *frq* mutants missing any of these elements (26) might be attributed to the removal of the WCC-interacting domain(s) or pleiotropic effects caused by polypeptide shortening. To address this, we engineered a set of *frq* mutants each missing ∼50 amino acids situated in these regions. In these mutants, *frq* transcription as reported by a *C-box*–driven *luciferase* gene whose product was measured in real-time (Fig. 1). $frq^{\Delta 564-603}$ shows a wildtype (WT) period length; $frq^{\Delta 691-732}$ displays a shortened period of 15.5 h; $frq^{\Delta 107-148}$, $frq^{\Delta 435-481}$, $frq^{\Delta 604-646}$, $frq^{\Delta 874-884}$, and $frq^{\Delta 857-905}$ have prolonged rhythms to variable extents. The core clock became totally arrhythmic in $frq^{\Delta 149-193}$, $frq^{\Delta 194-199}$, $frq^{\Delta 200-249}$, $frq^{\Delta 250-310}$, $frq^{\Delta 482-510,}$ $frq^{\Delta 511-558}$, $frq^{\Delta 647-690}$, $frq^{\Delta 733-774}$, $frq^{\Delta 775-800}$, and $frq^{\Delta 801-856}$. The data support the idea that multiple regions of FRQ take part in the rhythmicity control and period determination, as has been documented by a large body of literature.

FRQ–WCC integrity is affected in most arrhythmic strains

To examine the FFC–WCC formation that functions as the initial step in the repression elicited by FFC on WCC, FRQ (tagged with V5H6) in the *frq* mutants whose circadian phenotypes were analyzed by the luciferase assay in Figure 1 was pulled down with V5 resin, and FRQ, FRH, WC-1, and WC-2 were blotted with protein-specific antibodies (Fig. 2). The diffuse band of FRQ derived from multisite phosphorylations has been observed characteristically (32) from all the *frq* mutants that were grown in the light and tested (Fig. 2). When FRQ was enriched by immunoprecipitation (IP) in $frq^{\Delta 149-193}$, $frq^{\Delta 194-199}$, $frq^{\Delta 200-249}$, $frq^{\Delta 482-510,}$ $frq^{\Delta 511-558}$, $frq^{\Delta 647-690}$, $frq^{\Delta 733-774}$, $frq^{\Delta 775-800}$, $frq^{\Delta 801-856}$, and $frq^{\Delta 857-905}$, WC-1 and WC-2 became undetectable relative to the WT, and all except $frq^{\Delta 857-905}$ showed an arrhythmic clock and enhanced *C-box*-driven reporter activity (Figs. 1 and 2). FRQ–WCC is almost completely lost in $frq^{\Delta 857-905}$, but the mutant strain still showed a rhythm with prolonged period length (Figs. 1 and 2), suggesting that a stable FFC–WCC supercomplex is not required for the execution of the circadian feedback loop. $frq^{\Delta 107-148}$, $frq^{\Delta 564-603}$, $frq^{\Delta 604-646}$, and $frq^{\Delta 691-732}$ displayed weak FFC and WCC interaction but sustained weak rhythmicity (Figs. 1 and 2). This result confirms that multiple domains on FRQ contribute cooperatively to contact with WCC. FRH dissociates from FRQ in $frq^{\Delta 733-774}$, $frq^{\Delta 775-800}$, and $frq^{\Delta 801-856}$ (Fig. 2), which may lead to the loss of WCC in the complex as noted previously for *frq* mutants frq^{6B2} and frq^{6B5} (26). This also reinforces that FRQ needs to form a complex with FRH in order to interact with WCC (7, 8, 26), presumably through constructing a proper quaternary structure of FFC. The clock in $frq^{\Delta 733-774}$, $frq^{\Delta 775-800}$, and $frq^{\Delta 801-856}$ does not oscillate (Fig. 1), consistent with the finding that the absence of FRH in the FFC abrogates feedback loop closure (7, 8). $frq^{\Delta 250-310}$, $frq^{\Delta 435-481}$, and $frq^{\Delta 874-884}$ have normal FFC–WCC interaction (Fig. 2). Interestingly, although the interaction of FFC and WCC in $frq^{\Delta 250-310}$ seems unaffected, or even slightly stronger relative to WT (upper left in Fig. 2), the mutant is arrhythmic (Fig. 1), which might be due to an indirect impact of the deletion on the nearby FRQ-CK1 interacting domain (FCD-1) that has been shown to be essential for the clock (25). Collectively, the data here further characterize FRQ's regions involved in WCC interaction but suggest that the binding strength of FFC–WCC is not indicative of the period length.

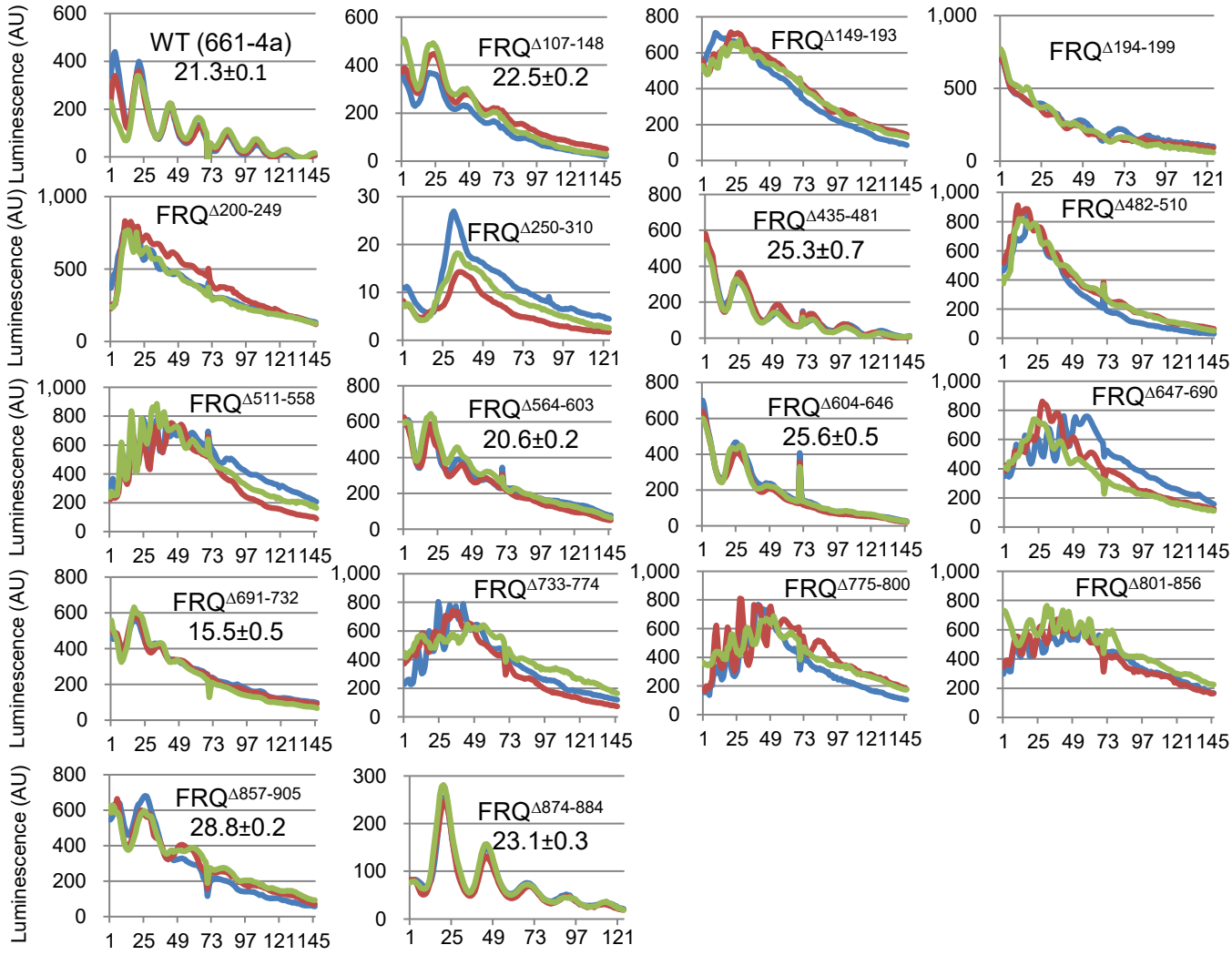

Figure 1. Luciferase assays of *frq* partial-deletion mutants grown at 25 °C in the dark. Strains were synchronized at 25 °C in the light overnight, and bioluminescence signals were tracked every hour by a CCD (charge-coupled device) camera after moving the strains to the dark at the same temperature. Three replicates (lines in different colors) were plotted for each mutant with the x-axis and y-axis representing time (in hours) and arbitrary units of the signal intensity, respectively. In this and subsequent figures, period length was calculated from three or more replicates and reported as the average ± the standard error of the mean (SEM). All *frq* mutants throughout this study were targeted to the native locus with a tandem V5 and 6× histidine (V5H6) tag at their C termini. FRQ, FREQUENCY.

FFC–WCC interaction can be disrupted by high salt

A basic stretch (KKKRKRRK) near the ZnF DNA-binding domain of WC-1 was previously identified as required for the WCC–FFC organization (21), which suggests that ionic charges may drive the complex formation. To confirm this hypothesis, the NaCl concentration in the standard protein–lysis buffer was raised from 137 mM that is used commonly in the biochemical analysis of FFC and WCC to 500 and 1000 mM, either WC-1 or FRQ was immunoprecipitated, and the four clock components followed subsequently by Western blotting. Following WC-1 IP, the enrichment of WC-2 was barely affected by high salts in the buffer, but FRQ and FRH were undetected when 500 mM or 1000 mM sodium chloride was used (Fig. 3*A*). Similarly, in a separate experiment with epitope-tagged FRQ instead, FRQ^{V5H6} as well as bound FRH were immunoprecipitated readily with V5 antibody regardless of salt titers, whereas WC-1 and WC-2 disappeared from the FFC when salt dosages rose (Fig. 3*B*). The data support that FFC and WCC associate with each other by virtue of electrostatic forces, which are subject to high salt disruptions *in vitro*, while WC-1 and WC-2 bind together presumably by hydrophobic effects *via* their PAS domains (26); likewise, both FRQ and FRH possess specified domains buttressing their interaction (26, 33). Accordingly, interactions between FRQ and FRH as well as WC-1 and WC-2 are less prone to high ionic strength disruptions.

Luciferase analysis of frq *D/E-to-A mutants*

Based on the observations that the organization of WCC–FFC is susceptible to the ambient ionic strength (Fig. 3) and also that the basic motif of WC-1 is needed for the WCC–FFC connection (21), negatively charged residues, Asp (D)/Glu (E), in the key regions of FRQ (Figs. 1 and 2) were mutated individually or in clusters to alanines for the purpose of pinning

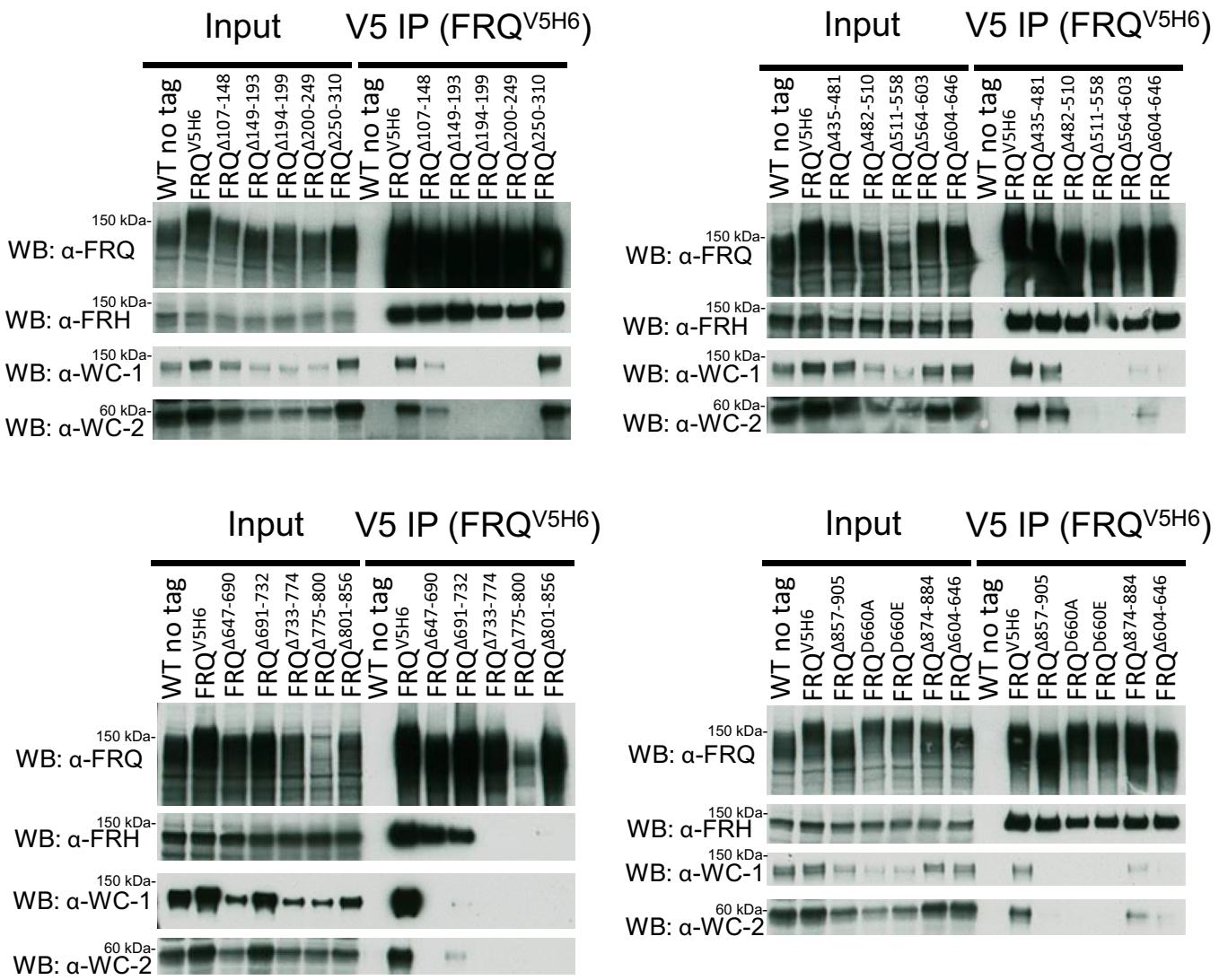

Figure 2. FRQ/FRH and WC-1/WC-2 interaction in the *frq*-partial-deletion mutants. FRQ (tagged with V5H6) was pulled down with V5 resin from a culture grown in constant light at 25 °C for 24 h, and Western blotting (WB) was carried out using custom antibodies (raised from rabbits) against FRQ, FRH, WC-1, or WC-2 as indicated (see Experimental procedures for details). For V5 IP, WT (no tag) serves as the negative control, while WT FRQ tagged by V5H6 (FRQ^{V5H6}) is the positive control. For "input", 15-μg total protein was loaded per lane, and 10 μl out of a total of 100 μl eluate was loaded per lane for "V5 IP" samples. In this and subsequent WB-based analyses, comparable results were obtained in multiple biological replicate experiments. FRH, FRQ-interacting RNA helicase; FRQ, FREQUENCY; WC-1, White Collar-1; WC-2, White Collar-2.

down (tagged) FRQ's residues involved in WCC binding. In subsequent luciferase reporter analyses, four classes of rhythm alterations were noted in these *frq* D/E-to-A mutants (Fig. 4): The clock became fully arrhythmic in $frq^{D149A,\ D150A,\ D156A,\ D157A}$, $frq^{E200A,\ E202A,\ D207A}$, $frq^{E760A,\ E763A,\ D773A,\ D774A}$, $frq^{E801A,\ D802A,\ E805A,\ E809A}$, and frq^{E835A}; period length was almost unaffected in $frq^{D664A,\ D667A}$, $frq^{E679A,\ E681A}$, $frq^{D687A,\ E688A,\ E690A}$, $frq^{D862A,\ D866A,\ D867A,\ D869A,\ D870A}$, $frq^{D874A,\ D875A,\ E876A,\ E877A,\ E879A,\ E880A,\ E882A,\ E883A,\ D884A}$, $frq^{E161A,\ E167A,\ E168A}$, and frq^{D243A}; $frq^{D738A,\ E739A,\ D740A,\ E747A,\ D748A}$ and $frq^{E888A,\ D901A}$ display decreased period lengths of 16.8 and 19.6 h respectively; period length of the rhythms was elongated by ∼2, 3, 5, and 7 h in $frq^{D214A,\ E217A}$, $frq^{E552A,\ D553A,\ E555A,\ D556A}$, $frq^{D532A,\ D539A,\ E542A,\ D543A}$, and $frq^{E511A,\ D521A}$, respectively. The data of period changes here agree fairly well with the period-alternating pattern of *frq* mutants from a recent publication demonstrating that mutating phosphorylation sites in the N terminal and middle regions of FRQ results typically in prolonged period lengths, while elimination of C-terminal phosphorylation events always lessens the period length (28). In $frq^{E801A,\ D802A,\ E805A,\ E809A}$, the level of FFC–WCC interaction is comparable to that in WT (Fig. 5), but the mutant strain was still arrhythmic in the luciferase assay (Fig. 4), suggesting that stable interaction between FFC and WCC is not sufficient for sustaining rhythmicity but instead transient but dynamic *in vivo* contacts between the two complexes may be required for the efficient and persistent inhibition of WCC, especially to the fraction of WCC that associates with the *C box* of the *frq* promoter.

The FFC–WCC establishment is impaired in certain frq *D/E-to-A mutants*

To determine whether the FFC–WCC in the D/E-to-A mutants from Figure 4 remains intact biochemically, we

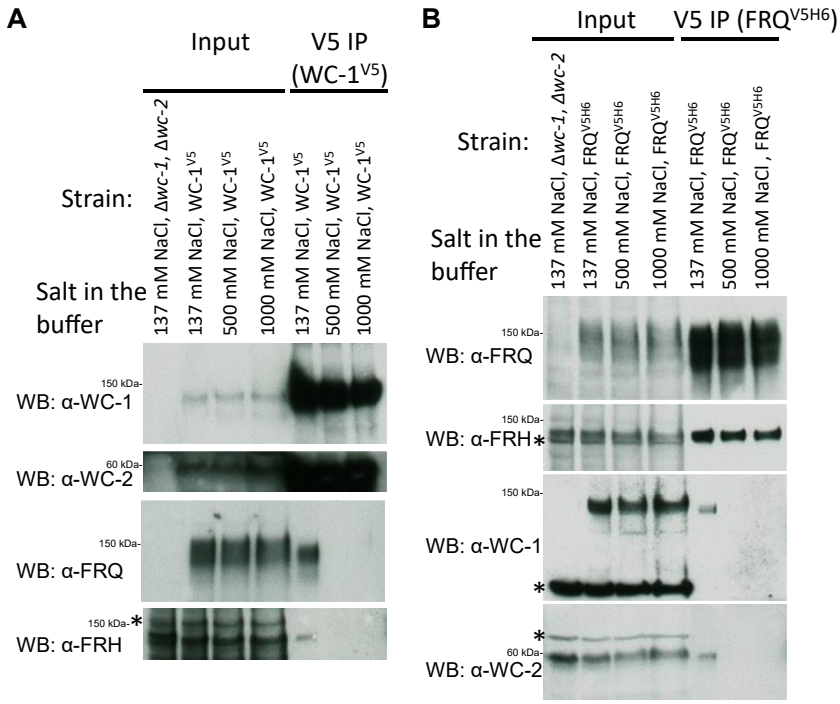

Figure 3. Increased salt concentration in the lysis/IP buffer disrupts the FFC-WCC complex. For IP (details can be found in Experimental procedures), the NaCl concentration in the lysis and wash buffers was set at 137, 500, or 1000 mM as indicated above the panel. *A*, WC-1^{V5} was cultured in the light at 25 °C for 24 h, harvested, and ground to a fine powder; buffers containing 137, 500, or 1000 mM NaCl were added respectively to the ground powder for cell lysis; centrifugation-cleared lysate was incubated with V5 resin in a volume of 1 ml of the same lysis and wash buffer to pull down WC-1^{V5}. Following IP, WB was carried out with WC-1-, WC-2-, FRQ-, or FRH-specific antibody as indicated. *B*, the strain of FRQ^{V5H6} was grown at 25 °C plus light for ∼24 h, and FRQ^{V5H6} was pulled down with V5 resin. For both (*A*) and (*B*), 15-μg total protein was loaded per "input" lane, while each "V5 IP" lane contained 10 μl eluate out of a total of 100 μl. Δ*wc-1*, Δ*wc-2* serves as the negative control. FFC, FRQ–FRH complex; FRH, FRQ-interacting RNA helicase; FRQ, FREQUENCY.

examined expression and interaction of the four core-clock components, FRQ, FRH, WC-1, and WC-2 by IP and Western blotting. FRQ was not detected in *frq*$^{D149A,\ D150A,\ D156A,\ D157A}$ and *frq*^{E835A} and was only very weakly detected in *frq*$^{E760A,\ E763A,\ D773A,\ D774A}$ after enrichment (Fig. 5), suggesting that mutations of these four residues may significantly impact FRQ stability; this explains why they displayed arrhythmicity but high signal intensity in the luciferase analysis (Fig. 4), basically mirroring the behavior of Δ*frq* or *frh* mutants (7, 8, 34). FRQ abundance in *frq*$^{E200A,\ E202A,\ D207A}$ drops drastically, which might lead to a reduction of FRH in the complex. The observations of little to no expression of FRQ along with diminished abundance of WCC in *frq*$^{D149A,\ D150A,\ D156A,\ D157A}$, *frq*$^{E200A,\ E202A,\ D207A}$, *frq*$^{E760A,\ E763A,\ D773A,\ D774A}$, and *frq*^{E835A} are nicely compatible with the "black widow model" proposing a negative correlation between the activity of transcription factors in transcription with their cellular abundance (8, 11, 35). Interestingly, WC-1 and WC-2 levels in the FFC–WCC in *frq*$^{D664A,\ D667A}$, *frq*$^{D862A,\ D866A,\ D867A,\ D869A,\ D870A}$, and *frq*$^{D874A,\ D875A,\ E876A,\ E877A,\ E879A,\ E880A,\ E882A,\ E883A,\ D884A}$ become dramatically reduced (can only be visualized with a long exposure in Western blotting) relative to WT, though FRQ and FRH in these strains interact normally with each other (Fig. 5). This result appears to be astonishing as the three *frq* mutants demonstrate an approximate WT period (Fig. 4), but it evidently suggests that the stability of the interaction between the positive and negative element complexes does not predict the period length and also suggests that FRQ-promoted phosphorylation of WCC can persist efficiently even with less WCC bound in the complex.

The third cluster of D/E on FRQ crucial for the WCC–FFC formation

FRQ was completely undetectable in *frq*$^{D149A,\ D150A,\ D156A,\ D157A}$, *frq*$^{E760A,\ E763A,\ D773A,\ D774A}$, and *frq*^{E835A} (Fig. 5). To probe the role of these D/E clusters, we made *frq* mutants bearing fewer mutations at these sites, or an E835D substitution, and monitored *C-box* activity and WCC–FFC establishment. FRQ's E183 and E187 were also included in the mutagenesis because they are located nearby D149, D150, D156, and D157. The clock in *frq*$^{D149A,\ D150A}$, *frq*$^{E760A,\ E763A}$, and *frq*^{E835D} oscillates robustly with an approximate WT period, while *frq*$^{D156A,\ D157A}$, *frq*$^{E183A,\ E187A}$, and *frq*$^{D773A,\ D774A}$ completely lost rhythmicity (*frq*$^{E183A,\ E187A}$ only shows one peak) (Fig. 6*A*). FRQ expression in *frq*$^{D773A,\ D774A}$ is extraordinarily low (a faint band after IP) (Fig. 6*B*), explaining the arrhythmicity in the luciferase assay (Fig. 6*A*). WC-1 and WC-2 levels in FFC–WCC became greatly diminished in *frq*$^{D149A,\ D150A}$, once again showing that the WCC–FFC abundance in the cell does not faithfully reflect the period length (Fig. 5). The loss of FFC–WCC in *frq*$^{E183A,\ E187A}$ and *frq*$^{D773A,\ D774A}$ (Fig. 6*B*) is consistent with abolished rhythmicity (Fig. 6*A*). These data reinforce the necessity of incorporating FFC into WCC for eliciting phosphorylation-induced repression. It is noteworthy that unlike *frq*^{E835A} in which FRQ protein

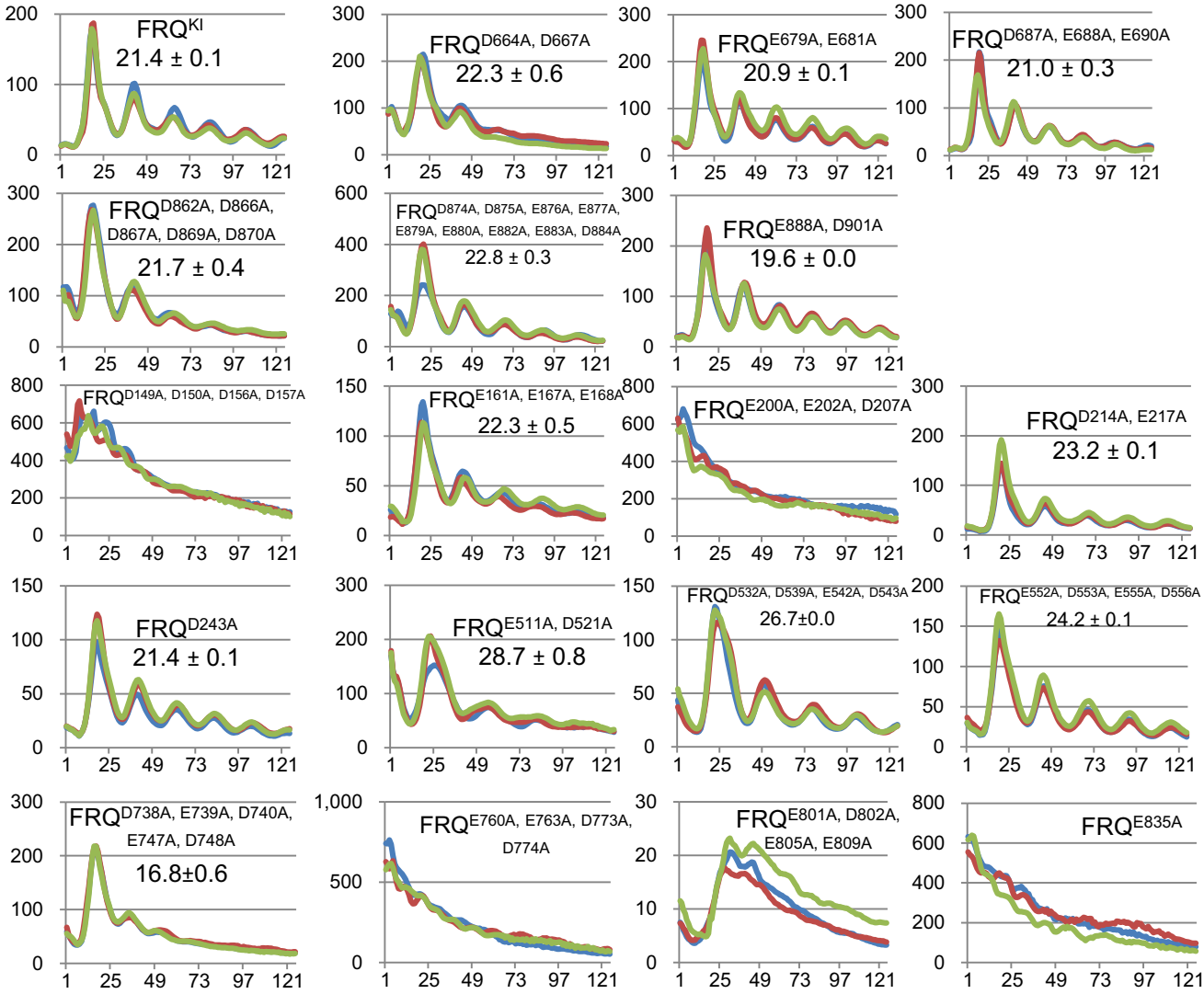

Figure 4. Luciferase assays of *frq* D/E-to-A mutants at 25 °C in the dark. Synchronization of strains was done in the light at 25 °C overnight, and light signals were tracked every hour by a CCD camera following the transfer of the strains to the dark at 25 °C. Lines in different colors represent three replicates with the x-axis and y-axis displaying time (in hours) and the signal intensity (arbitrary units), respectively. Period length was determined from three replicates and shown as the average ± the SEM. All *frq* mutants bear a V5H6 tag at their C termini, targeting at the *frq* native locus. CCD, charge-coupled device; FRQ, FREQUENCY.

accumulation was abolished (Fig. 5), frq^{E835D} bears a vigorously oscillating clock as well as normal FRQ abundance and unchanged interaction of FRQ with WCC and FRH in comparison with WT (Fig. 6*B*), suggesting that the negative charge of E835 is the main contributor in promoting FRQ accumulation.

Expression and clock-components interaction in frq *truncations*

Certain residues on FRQ, including D773, D774, and E835, contribute significantly to the accumulation of the full-length protein (Figs. 5 and 6). We wondered whether this observation also applies to truncated variants of FRQ and whether retaining certain clusters of important D/E suffices for WCC recruitment. Hence, we made two sets of *frq* mutants each bearing abridged versions of FRQ, and these truncated FRQ segments together cover all the residues of the full-length FRQ twice: $frq^{1–558}$ and $frq^{559–989}$, $frq^{1–310}$, $frq^{311–628}$, and $frq^{629–989}$ (Fig. 7*A*). As expected, $frq^{1–310}$, $frq^{311–628}$, and $frq^{629–989}$ totally lost rhythmicity in the luciferase assay (Fig. 7*A*). The FRQ level in $frq^{1–310}$ fell below our detection limit in Western blotting even after an enrichment by IP, while in other mutants, it appears to be comparable to that in WT (Fig. 7*B*). Although FRH complexed with FRQ as strongly in $frq^{559–989}$ and $frq^{629–989}$ as in WT, WC-1 and WC-2 in all of these mutants was undetectable above the background in Western blotting (Fig. 7*B*), indicating that preservation of individual D/E clusters is not sufficient for FFC–WCC formation.

Glu (E) substitution of FRQ's D660 phenocopies frq^{D660A}

FRQ's residue D660 was found to be essential for FFC to recruit WCC and thereby for the negative feedback loop (36). To test whether retaining the negative charge of D660

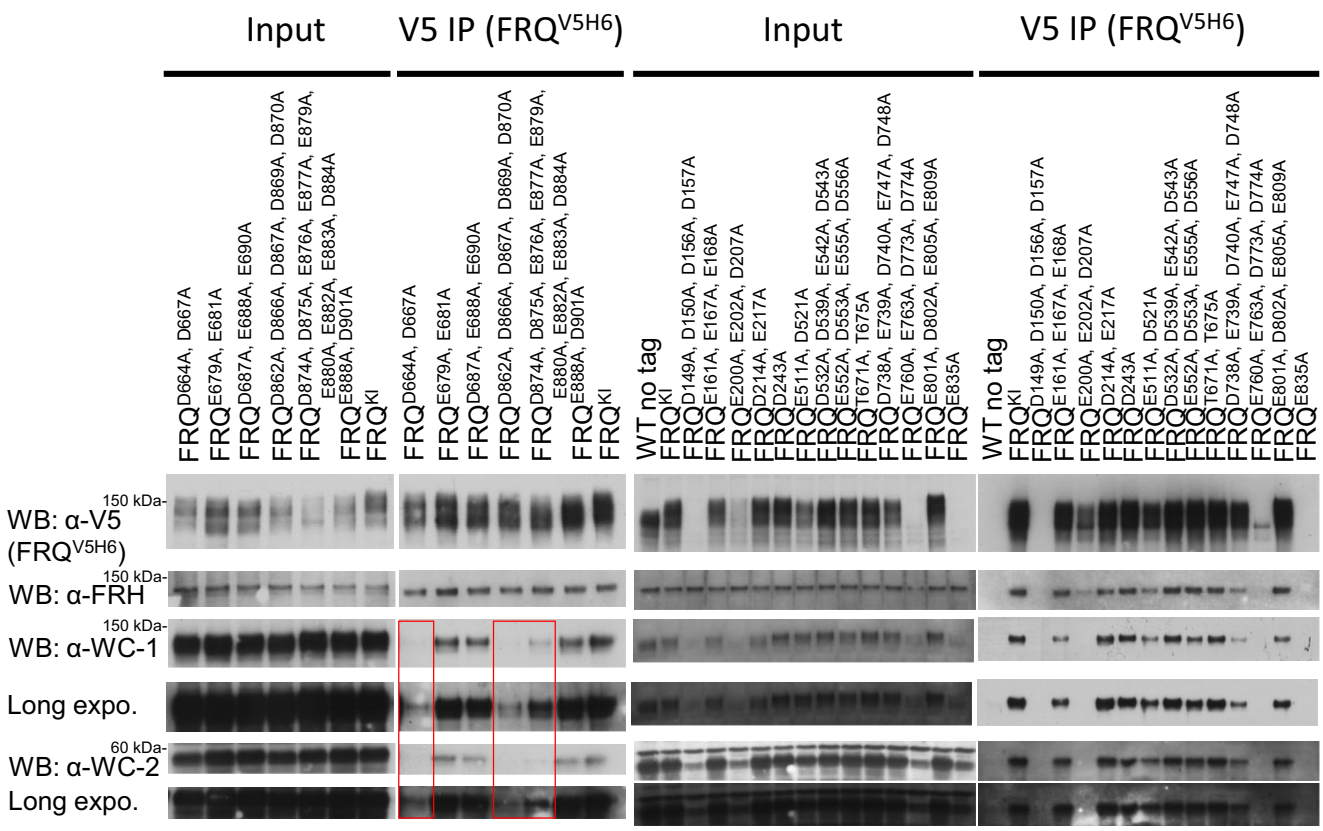

Figure 5. Two clusters of D/E in the C terminus of FRQ are essential for associating with WCC. FRQ (bearing a V5H6 tag) was pulled down with V5 resin from a culture grown in constant light at 25 °C, and WB was performed using antibodies against FRQ, FRH, WC-1, or WC-2 as indicated. WT FRQ tagged by V5H6 (FRQ^{V5H6}) is the positive control in the assay. *Red boxes* mark the absence of, or an extremely reduced amount of, FFC-bound WCC. FFC, FRQ–FRH complex; FRH, FRQ-interacting RNA helicase; FRQ, FREQUENCY; WC-1, White Collar-1; WC-2, White Collar-2; WCC, White Collar complex.

preserves the role of FRQ in the clock, we generated frq^{D660E} and assayed it for *C-box* activity by luciferase analysis and WCC interaction by IP. To our surprise, frq^{D660E} behaved as arrhythmically as frq^{D660A} (Fig. 8*A*) and failed to rescue the loss of the FFC–WCC in frq^{D660A} (Fig. 1). The data reveal that the negative charge of D660 is not the sole factor in determining the FFC–WCC formation and circadian rhythmicity, an observation that contrasts sharply with what we have obtained from frq^{E835A} and frq^{E835D} (Figs. 5 and 6), demonstrating the importance of the side-chain charge of E835 in promoting FRQ accumulation. The intramolecular interaction between the N and C termini of FRQ has been noticed (25). E835 may be involved in the binding of the C-terminal tail of FRQ with its N terminus.

Discussion

In *Neurospora*, the *frequency* gene encodes the central scaffolding protein FRQ that organizes the multicomponent negative arm of the core clock, and the cellular timing information has been encoded sophisticatedly and situated precisely in its expression and probably more importantly in its chemical modifications. Unfortunately, the complete FRQ structure, like that of its mammalian counterparts the PERs, remains unresolved due mainly to its low abundance in the cell and intrinsically disordered nature. This leaves many questions concerning the core-clock operation unsettled. For instance, how do the negative arm complexes FFC and PERs/CRYs accurately bridge kinases to progressively inhibit WCC or CLOCK/BMAL1 *via* phosphorylation in the repressive phase of the clock and how is it that FFC only binds to a small percentage of WCC but is able to proficiently repress all the WCC molecules in the cell. In this study, we attempted to probe these queries by searching for important regions and more specifically key residues of FRQ engaging in WCC contacts. Segment-deletion analysis identified regions on FRQ required for the core oscillator as well as WCC recruitment (Figs. 1 and 2). In agreement with prior literature, more than one region on FRQ contributes to WCC interaction (Fig. 2). Biochemical analysis further revealed that the FFC–WCC complex is vulnerable to elevated salt; the DBD on WC-1 was identified as a key for FFC interaction. Altogether, these leads guided us to dissect negatively charged residues falling in the regions of FRQ that were found to be important for WCC interaction (Fig. 1). In addition, we found residues vital for FRQ accumulation or stability as well as the ones significantly impacting period length when mutated (Fig. 4). IP assays confirmed that three clusters of negatively charged amino acids, D149/D150/D156/D157/E183/E187, D664/D667, and D/E from aa 862-D884 (Fig. 8*B*), are required for WCC

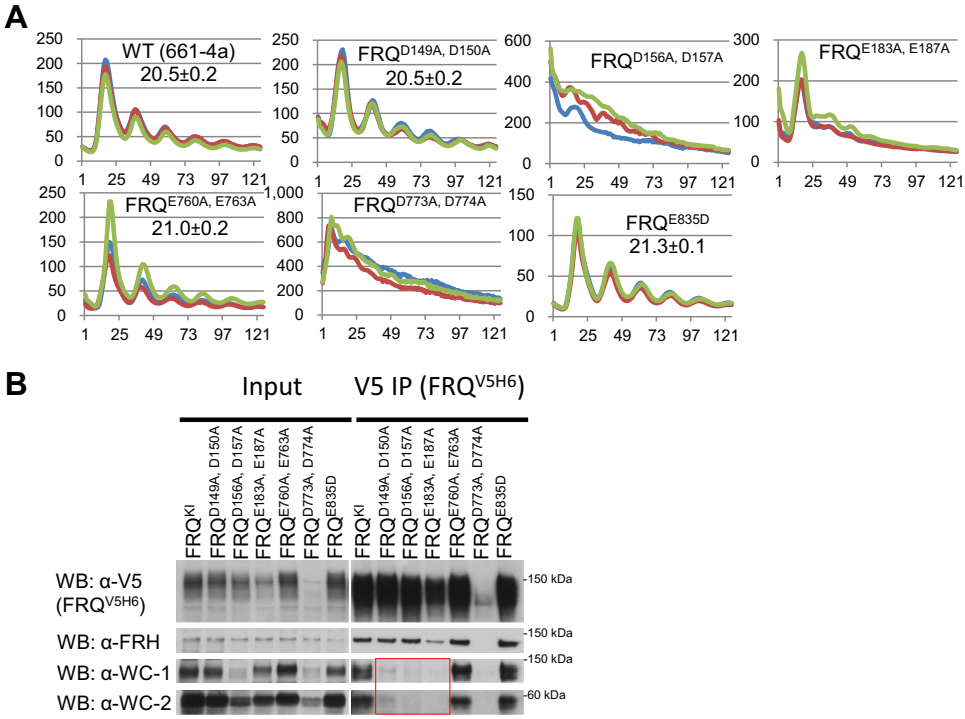

Figure 6. FRQ residues D149, D150, D156, D157, E183, and E187 are needed for FFC to bind WCC. *A*, luciferase assays of indicated *frq* mutants at 25 °C in the dark. Synchronization for the clock was carried out at 25 °C plus light overnight, cultures were transferred to the dark, and then bioluminescence signals from the dark-grown strains (at 25 °C) were tracked every hour. Three replicates are represented by differently colored lines with time (in hours) as the x-axis and the signal intensity (arbitrary units) as the y-axis. Period length was measured from three replicates and displayed as the average ± the SEM. All *frq* alleles were appended with a V5H6 tag at their C termini at the *frq* locus. *B*, interaction of clock components FRQ, FRH, WC-1, and WC-2 in the stated *frq* mutants. V5H6-tagged FRQ was immunoprecipitated with V5 resin from strains cultured in the light at 25 °C for ∼24 h, and WB was carried out with indicated antibodies against FRQ, FRH, WC-1, or WC-2 (see Experimental procedures for details). The *red box* denotes remarkably decreased or undetected WCC from the FRQ pull-down (by V5). FFC, FRQ–FRH complex; FRH, FRQ-interacting RNA helicase; FRQ, FREQUENCY; WC-1, White Collar-1; WC-2, White Collar-2; WCC, White Collar complex.

association, but surprisingly, $frq^{D664A,\ D667A}$, $frq^{D862A,\ D866A,\ D867A,\ D869A,\ D870A}$, and $frq^{D874A,\ D875A,\ E876A,\ E877A,\ E879A,\ E880A,\ E882A,\ E883A,\ D884A}$ displayed vigorous circadian rhythms with a period length almost identical to WT. These data indicate that the stability of the interaction between the positive and negative elements does not control the pace of the oscillator. It remains elusive whether the FRQ's D/E residues discovered in this study are located on the interface of the FRQ structure and contact the WCC directly or whether they contribute to the maintenance of FRQ's tertiary structures that are needed in WCC recognition.

Recently, the binding strength of FRQ-CK1 has been demonstrated to be an indicator of the period length at normal temperatures as well as in a physiological temperature range (37, 38). The correlation of WCC-FRQ abundance with period length is vague since *frq* mutants with a constant WCC-FRQ level showed varying period lengths (37). Most WCC in the cell resides in the nucleus, while the majority of FRQ is located in the cytoplasm (12, 21, 24, 31). These observations underpin the fact that even in the WT strain, only a small portion of the FFC pool encounters and then complexes with WCC (12). The FFC–WCC supercomplex (in terms of size) (12) may assemble in a dynamic manner as evidenced by the quantitative proteomic data showing that WCC interacts preferentially with hypophosphorylated FRQ, whereas FRH associates constantly with FRQ independent of the latter's phosphorylation status. Unexpectedly, we here saw that the period length in certain *frq* mutants was almost unaffected even with the severely impaired WCC–FFC establishment based on co-IP. Based upon prior evidence, this may be interpreted in several ways. First of all, there may be only a limited fraction of the WCC pool actively participating in *frq* transcription, and correspondingly timely expressed FRQ only needs to repress this small amount of DNA-bound WCC. Thus, the core oscillator could operate in a normal way even in mutants composed of markedly less FRQ and WCC (similar to the scenario in WT with most FFC and WCC not participating in the core oscillator). This has been suggested by experimental data showing that downregulation of WCC does not greatly perturb circadian rhythmicity beyond a slight ∼2 h period lengthening (35). Second, the dynamic organization of WCC–FFC may ensure that the clock can be sustained with less WCC and FFC involved. Previous findings suggested that both WCC and FRQ rapidly translocate between the nucleus and cytoplasm (39, 40). Finally, the course of FFC-mediated WCC repression *via* phosphorylation lasts more than roughly half a day (41, 42). Therefore, FFC in certain mutants may be still fully capable of bringing about sufficient inactivation to WCC over a long while, even though the inactivation efficiency may be not as high as that in WT. These possibilities need not be mutually

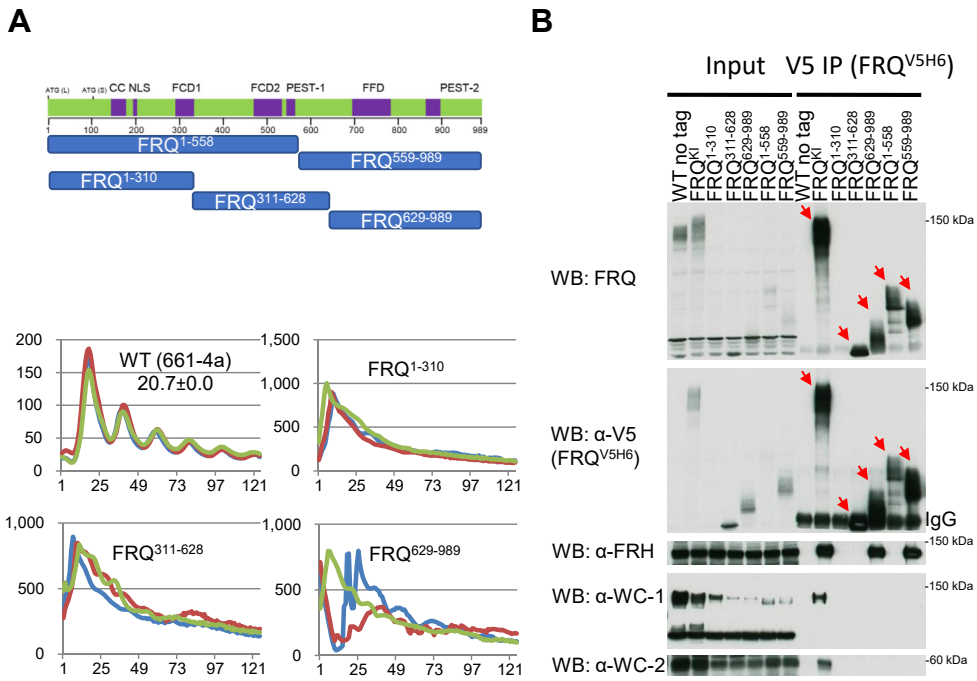

Figure 7. Truncated variants of FRQ have variable expression levels and WCC&FRH interactions. *A*, schematics of *frq* mutants covering different regions of the entire FRQ open-reading frame. *Upper*, each *blue bar* means a *frq* mutant encoding a polypeptide with the beginning and ending residues labeled within the bar. All *frq* mutants here carry a V5H6 at the C terminus just as others in this study. *Bottom*, luciferase analysis of $FRQ^{1–310}$, $FRQ^{311–628}$, and $FRQ^{629–989}$ strains that carry a *C-box* promoter-driven *luciferase* gene at 25 °C in the dark. *B*, expression and interaction of FRQ, FRH, WC-1, and WC-2 in the indicated *frq* mutants. Immunoprecipitation was done with V5 resin to pull down V5H6-tagged FRQ from strains cultured in the light at 25 °C for ∼24 h, and WB was carried out with indicated antibodies against FRQ, FRH, WC-1, or WC-2. *Red arrows* point to FRQ bands in V5 immunoprecipitations. Note: The FRQ band in $frq^{1–310}$ partially overlaps with the IgG band in the WB of V5 but is evident in the top blot with FRQ-specific antibody. FRH, FRQ-interacting RNA helicase; FRQ, FREQUENCY; WC-1, White Collar-1; WC-2, White Collar-2; WCC, White Collar complex.

exclusive, including that FFC may only need to repress DNA-bound WCC, and this process may proceed in a slow manner *in vivo*. Most likely, transient interaction between the two complexes may be sufficient for their recognitions and also for FFC-mediated repression of WCC *via* phosphorylation. Of course, the transient interaction might be affected in biochemical analyses, likely even from the point of the breaking up of a cell.

FRQ phosphorylation has been extensively explored for decades as the primary regulatory mechanism governing the *Neurospora* clock (10, 28–30, 43–50). Newly synthesized hypophosphorylated FRQ possesses higher affinity for WCC than the massively phosphorylated isoforms found at subsequent circadian times, implying that multisite phosphorylation events on FRQ modulate the FFC–WCC assembly. Phosphorylation of FRQ may negatively impact WCC's accessibility to certain important D/E residues of FRQ. Alternatively, mutations to these D/E residues may impinge on nearby phosphoevents, although we did not notice obvious alterations of the overall phosphorylation profiles of FRQ in these mutants (Figs. 5 and 6*B*). Strong defects in FRQ phosphorylation have been noticed in several *frq* mutants from this study, including $frq^{D773A,\ D774A}$ (Fig. 6*B*), $frq^{E760A,\ E763A,\ D773A,\ D774A}$ (the rightmost panel of Fig. 5), $frq^{\Delta775–800}$ (lower left of Fig. 2*A*), and $frq^{311–628}$ (Fig. 7*B*), which suggest that CK1 does not function normally in phosphorylating FRQ in these *frq* mutants given that CK1 is a stable component of FFC and also the major kinase in mediating FRQ phosphorylation (See the paragraph of "FRQ functions mainly as…"). In summary, we confirmed that multiple regions of FRQ are required for FFC to bind WCC and identified important negatively charged residues of FRQ required for WCC interaction.

Experimental procedures

Strains

Neurospora strain 661-4a ($ras\text{-}1^{bd}$, *A*, *his-3::C-box-driven luciferase*), which serves as WT in luciferase assays, contains the *frq C-box* promoter fused to the codon-optimized firefly *luciferase* (transcriptional fusion) at the *his-3* locus (41, 51).

frq *mutant generation*

frq mutants were created by a modified method using yeast homologous recombination-based integration of PCR fragments (28): Restriction-digested shuttle vector *pCB05* (10) was recombined with PCR (Thermo Fisher Scientific, Catalog # F549S) products amplified with primers bearing partial deletions or point mutations of FRQ. Four primer pairs worked as flanks in homologous recombination in a yeast strain (*FY834*). To introduce deletions falling in aa 1 to 214 of FRQ, two PCR reactions were performed: one with a forward primer "*frq* segment 1F" (5′-GAACCAGAACGTAGCAGTGTG-3′) and a reverse primer "del.aa # to # R" bearing a deletion to FRQ and the other using a forward primer "del.aa # to # F" which is reverse and complementary to "del.aa # to # R" and a reverse primer "*frq* segment 1R" (5′-GACGATGACGACGAATCGTG-3′), and

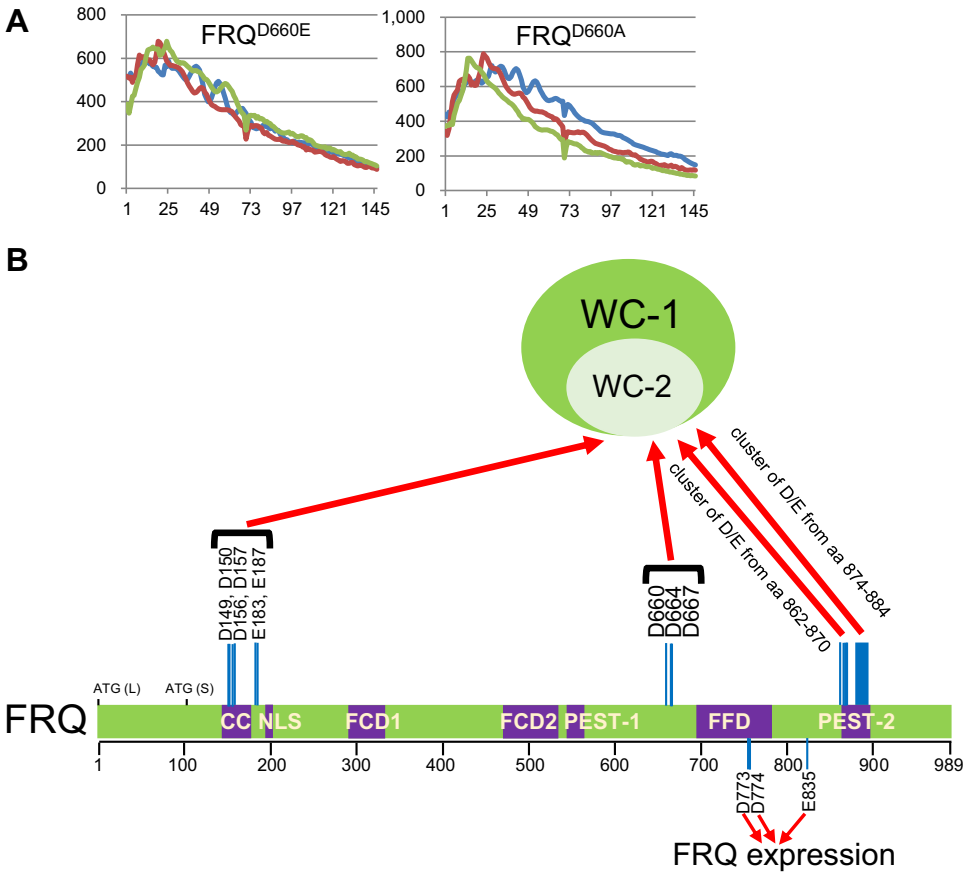

Figure 8. A working model illustrating FRQ's D/E clusters that mediate the WCC–FFC formation. *A*, luciferase analysis of FRQ^{D660A} and FRQ^{D660E}. Not all FFC–WCC interactions are electrostatic. Data here are presented in a similar manner as in prior figures with x- and y-axes representing hours and arbitrary units of the luminescence intensity respectively. *B*, a depiction summarizing the negatively charged residues (D and E) on FRQ in controlling WC-1 and WC-2 interaction. The cluster of D/E from amino acids 862 to 870 contains D862, D866, D867, D869, and D870; that from aa 874 to 884 includes residues D874, D875, E876, E877, E879, E880, E882, E883, and D884. The *red arrows* represent that these residues in FRQ contribute either directly (through physical contacts) or indirectly (such as constructing or maintaining regional structures) to binding WCC. CC, coiled-coil; FCD1, FRQ-CK-1a interaction domain 1; FCD2, FRQ-CK-1a interaction domain 2; FFC, FRQ–FRH complex; FRQ, FREQUENCY; NLS, nuclear localization signal; WCC, White Collar complex.

then, the two PCR products were cotransformed into yeast along with *pCB05* digested with *Bst*XI (New England Biolabs [NEB], Catalog # R0113S) and *Xho*I (NEB, Catalog # R0146S) to generate a circular construct. Likewise, for mutations falling in aa 215 to 437 of FRQ, primers "*frq* segment 2F" (5′-GTGA GTTGGAGGCAACGCTC-3′) and "*frq* segment 2R" (5′-GTC CATATTCTCGGATGGTA-3′ were used for PCRs in combination with *pCB05* digested with *Xho*I (NEB, Catalog # R0146S) to *Nru*I (NEB, Catalog # R0192S); "*frq* segment 3F" (5′-GTCG CACTGGTAACAACACCTC-3′) and "*frq* segment 3R" (5′-CA GCACATGTTCAACTTCATCAC-3′) were designed for *pCB05* digested with *Nru*I (NEB, Catalog # R0192S) and *Fse*I (NEB, Catalog # R0588S) (FRQ aa 438–675), and "*frq* segment 4F" (5′-CACCGATCTTTCAGGAGACCCTG-3′) and "*frq* segment 4R" (5′-CACTCAGGTC TCAATGGTGA TG-3′) pair with *pCB05* digested with *Fse*I (NEB, Catalog # R0588S) and *Mlu*I (NEB, Catalog # R0198S) (FRQ aa 676–989). If deleting regions or mutating residues involve two or more segments above, corresponding restriction enzymes and primers encompassing the regions were selected and combined for yeast recombination. All targeted mutations were validated by cycle sequencing with *frq*-specific primers at the Dartmouth Core facility. All these *frq* variants were targeted for homologous recombination at its native locus. Plasmids verified by Sanger sequencing were linearized with *Ase*I (NEB, Catalog # R0526S) and *Ssp*I (NEB, Catalog # R0132S) and purified with the QIAquick PCR Purification Kit (Qiagen, Catalog # 28104) for *Neurospora* transformation. *Neurospora* transformation *via* electroporation (settings: 1500 V, 600 Ω, and 25 μF) was performed using an electroporator (BTX, Model # ECM 630) as previously reported (52). The recipient strain for generating *frq* mutants is Δ*frq::hph*; Δ*mus-52::hph*; *ras-1^{bd}*; *C-box luciferase at his-3*, and all *frq*-mutant strains made in this research bear the *ras-1^{bd}* mutation (53) and *frq C-box*-driven codon-optimized firefly *luciferase* gene at the *his-3* locus for phenotype analyses, and they also contain a V5H6 tag at their C termini for biochemical assays.

Growth conditions

All vegetative cultures were maintained on complete-medium slants bearing 1× Vogel's, 1.6% glycerol, 0.025% casein hydrolysate, 0.5% yeast extract, 0.5% malt extract, and 1.5% agar (54). *Neurospora* sexual crosses were performed on

Westergaard's agar plates containing 1× Westergaard's salts, 2% sucrose, 50 ng/ml biotin, and 1.5% agar (55). For luciferase assays, strains were grown in the race-tube medium (1× Vogel's salts, 0.17% arginine, 1.5% bacto-agar, 50 ng/ml biotin, and 0.1% glucose) plus 12.5 μM luciferin (GoldBio, Catalog # LUCK-2G) in the light at 25 °C overnight, and bioluminescence signals were monitored hourly by a charge-coupled device camera in the dark at 25 °C. For IP assays examining WCC and FFC interaction, strains were cultured in the liquid culture medium (1× Vogel's, 0.5% arginine, 50 ng/ml biotin, and 2% glucose) with shaking at 125 rpm in the light at 25 °C overnight.

Protein lysate and Western blot

Protein lysates for Western blots (WBs) were prepared as previously described (56, 57). Liquid medium for culturing *Neurospora* is composed of 1× Vogel's, 0.5% arginine, 50 ng/ml biotin, and 2% glucose. Vacuum-dehydrated *Neurospora* tissue was frozen thoroughly in liquid nitrogen and ground to a fine powder using a mortar and pestle, the protein-extraction buffer (50 mM Hepes [pH 7.4], 137 mM NaCl, 10% glycerol, 0.4% NP-40) with cOmplete, Mini, EDTA-free Protease Inhibitor Cocktail (Roche, Catalog # 04693159001, at a dilution of one tablet to 10 ml buffer) was added to the powder, and the mixture of the *Neurospora* tissue powder and buffer was treated with cycles of vortexing for 10 s and resting on ice for another 10 s for a total of 2 min. For WB, equal amounts (15 μg) of centrifugation (12,000 rpm at 4 °C for 10 min)-cleared whole-cell lysate were loaded per lane in a commercial 3 to 8% 1.5-mm × 15-well Tris-Acetate SDS gel (Thermo Fisher Scientific, Catalog # EA03785BOX) with 1× NuPAGE Tris-Acetate SDS Running Buffer (Thermo Fisher Scientific, Catalog # LA0041). Rabbit V5 antibody (Abcam, Catalog # ab9116), mouse FLAG antibody (Sigma-Aldrich, Catalog # F3165), or rabbit HA (Abcam, Catalog # ab9110) was diluted at 1:5000 as the primary antibodies (48). Custom rabbit FRQ, FRH, WC-1, and WC-2 antibodies have been described previously for applications in WB (6, 32, 58).

Immunoprecipitation

IP with *Neurospora* lysate was performed as previously described (21). Briefly, 2 mg of total protein (cleaned by 12,000 rpm centrifugation at 4 °C for 10 min) were incubated with 20 μl of V5 agarose (Sigma-Aldrich, Catalog #7345) by rotating at 4 °C for 2 h. The agarose beads were then washed twice with the same protein extraction buffer (50 mM Hepes [pH 7.4], 137 mM NaCl, 10% glycerol, 0.4% NP-40) and eluted by adding 100 μl of 5 × SDS sample buffer and then being heated at 99 °C for 5 min. Ten out of the 100 μl IP were loaded per lane in WB.

Luciferase assays

Luciferase assays were performed as previously described (59, 60). 96-well plates with each well containing 0.8 ml of the luciferase-assay medium were inoculated with conidial suspension, and the inoculated strains were grown at 25 °C plus constant light for 16 to 24 h and then transferred to the dark at the same temperature for recording the light production. Bioluminescence signals were recorded with a charge-coupled device camera every hour, data were obtained with ImageJ and a custom macro, and period lengths of the strains were manually calculated. Raw data from three replicates were shown in the figures, and time (in hours) is on the x-axis, while arbitrary units of the signal intensity are on the y-axis. Medium for luciferase assays contains 1× Vogel's salts, 0.17% arginine, 1.5% bacto-agar, 50 ng/ml biotin, 0.1% glucose, and 12.5 μM luciferin (GoldBio, Catalog # LUCK-2G). WT used in luciferase assays was 661-4a (*ras-1^{bd}*, *A*) containing the *frq C-box* fused to the codon-optimized firefly *luciferase* gene (transcriptional fusion) at the *his-3* locus.

Data availability

The *Neurospora* strains made in this study are available upon request. All data used to draw conclusions of the article have been presented within the figures.

Author contributions—B. W. conceptualization; B. W. methodology; B. W. software; B. W. validation; B. W. formal analysis; B. W. investigation; B. W. writing–original draft; B. W. visualization; J. C. D. resources, J. C. D. writing–review & editing; J. C. D. funding acquisition.

Funding and additional information—This work was funded by the National Institutes of Health to Jay C. Dunlap (R35GM118021). Sequencing was performed in Dartmouth core facilities supported by the Dartmouth Cancer Center and by COBRE 5P20GM130454. The content is solely the responsibility of the authors and does not necessarily represent the official views of the National Institutes of Health.

Conflict of interest—The authors declare that they have no conflicts of interest with the contents of this article.

Abbreviations—The abbreviations used are: CK1, casein kinase 1; CRYs, CRYPTOCHROMEs; DBD, defective in DNA binding; FFC, FRQ–FRH complex; FRH, FRQ-interacting RNA helicase; FRQ, FREQUENCY; PAS, Per-Arnt-Sim; PERs, PERIODs; WB, Western blots; WC-1, White Collar-1; WCC, White Collar complex; ZnF, zinc finger.

References

1. Liu, Y. (2003) Molecular mechanisms of entrainment in the *Neurospora* circadian clock. *J. Biol. Rhythms* **18**, 195–205
2. Liu, Y., and Bell-Pedersen, D. (2006) Circadian rhythms in *Neurospora crassa* and other filamentous fungi. *Eukaryot. Cell* **5**, 1184–1193
3. Bell-Pedersen, D., Cassone, V. M., Earnest, D. J., Golden, S. S., Hardin, P. E., Thomas, T. L., *et al.* (2005) Circadian rhythms from multiple oscillators: lessons from diverse organisms. *Nat. Rev. Genet.* **6**, 544–556
4. He, Q., Cheng, P., Yang, Y., Wang, L., Gardner, K. H., and Liu, Y. (2002) White collar-1, a DNA binding transcription factor and a light sensor. *Science* **297**, 840–843
5. Froehlich, A. C., Loros, J. J., and Dunlap, J. C. (2003) Rhythmic binding of a WHITE COLLAR-containing complex to the *frequency* promoter is inhibited by FREQUENCY. *Proc. Natl. Acad. Sci. U. S. A.* **100**, 5914–5919

6. Froehlich, A. C., Liu, Y., Loros, J. J., and Dunlap, J. C. (2002) White Collar-1, a circadian blue light photoreceptor, binding to the *frequency* promoter. *Science* **297**, 815–819
7. Cheng, P., He, Q., He, Q., Wang, L., and Liu, Y. (2005) Regulation of the *Neurospora* circadian clock by an RNA helicase. *Genes Dev.* **19**, 234–241
8. Shi, M., Collett, M., Loros, J. J., and Dunlap, J. C. (2010) FRQ-interacting RNA helicase mediates negative and positive feedback in the *Neurospora* circadian clock. *Genetics* **184**, 351–361
9. [preprint] Jankowski, M. S., Griffith, D., Shastry, D. G., Pelham, J. F., Ginell, G. M., Thomas, J., *et al.* (2022) The formation of a fuzzy complex in the negative arm regulates the robustness of the circadian clock. *bioRxiv*. https://doi.org/10.1101/2022.01.04.474980
10. Sweeney, B. M., and Hastings, J. W. (1960) Effects of temperature upon diurnal rhythms. *Cold Spring Harb. Symp. Quant. Biol.* **25**, 87–104
11. Wang, B., Kettenbach, A. N., Zhou, X., Loros, J. J., and Dunlap, J. C. (2019) The phospho-code determining circadian feedback loop closure and output in *Neurospora*. *Mol. Cell* **74**, 771–784
12. Schafmeier, T., Haase, A., Káldi, K., Scholz, J., Fuchs, M., and Brunner, M. (2005) Transcriptional feedback of *Neurospora* circadian clock gene by phosphorylation-dependent inactivation of its transcription factor. *Cell* **122**, 235–246
13. Mohawk, J. A., Green, C. B., and Takahashi, J. S. (2012) Central and peripheral circadian clocks in mammals. *Annu. Rev. Neurosci.* **35**, 445–462
14. Cao, X., Yang, Y., Selby, C. P., Liu, Z., and Sancar, A. (2021) Molecular mechanism of the repressive phase of the mammalian circadian clock. *Proc. Natl. Acad. Sci. U. S. A.* **118**, e2021174118
15. Michael, A. K., Fribourgh, J. L., Chelliah, Y., Sandate, C. R., Hura, G. L., Schneidman-Duhovny, D., *et al.* (2017) Formation of a repressive complex in the mammalian circadian clock is mediated by the secondary pocket of CRY1. *Proc. Natl. Acad. Sci. U. S. A.* **114**, 1560–1565
16. Parico, G. C. G., Perez, I., Fribourgh, J. L., Hernandez, B. N., Lee, H.-W., and Partch, C. L. (2020) The human CRY1 tail controls circadian timing by regulating its association with CLOCK:BMAL1. *Proc. Natl. Acad. Sci. U. S. A.* **117**, 27971–27979
17. Gustafson, C. L., Parsley, N. C., Asimgil, H., Lee, H.-W., Ahlbach, C., Michael, A. K., *et al.* (2017) A slow conformational switch in the BMAL1 transactivation domain modulates circadian rhythms. *Mol. Cell* **66**, 447–457.e7
18. Ye, R., Selby, C. P., Chiou, Y.-Y., Ozkan-Dagliyan, I., Gaddameedhi, S., and Sancar, A. (2014) Dual modes of CLOCK:BMAL1 inhibition mediated by cryptochrome and period proteins in the mammalian circadian clock. *Genes Dev.* **28**, 1989–1998
19. Rojas, V., Salinas, F., Romero, A., Larrondo, L. F., and Canessa, P. (2022) Interactions between core elements of the *Botrytis cinerea* circadian clock are modulated by light and different protein domains. *J. Fungi (Basel)* **8**, 486
20. Cheng, P., Yang, Y., Gardner, K. H., and Liu, Y. (2002) PAS domain-mediated WC-1/WC-2 interaction is essential for maintaining the steady-state level of WC-1 and the function of both proteins in circadian clock and light responses of *Neurospora*. *Mol. Cell Biol* **22**, 517–524
21. Wang, B., Zhou, X., Loros, J. J., and Dunlap, J. C. (2016) Alternative use of DNA binding domains by the *Neurospora* White Collar complex dictates circadian regulation and light responses. *Mol. Cell. Biol.* **36**, 781–793
22. Cha, J., Zhou, M., and Liu, Y. (2015) Mechanism of the *Neurospora* circadian clock, a FREQUENCY-centric view. *Biochemistry* **54**, 150–156
23. Cheng, P., Yang, Y., Heintzen, C., and Liu, Y. (2001) Coiled-coil domain-mediated FRQ-FRQ interaction is essential for its circadian clock function in *Neurospora*. *EMBO J.* **20**, 101–108
24. Luo, C., Loros, J. J., and Dunlap, J. C. (1998) Nuclear localization is required for function of the essential clock protein FRQ. *EMBO J.* **17**, 1228–1235
25. Querfurth, C., Diernfellner, A. C. R., Gin, E., Malzahn, E., Höfer, T., and Brunner, M. (2011) Circadian conformational change of the *Neurospora* clock protein FREQUENCY triggered by clustered hyperphosphorylation of a basic domain. *Mol. Cell* **43**, 713–722
26. Guo, J., Cheng, P., and Liu, Y. (2010) Functional significance of FRH in regulating the phosphorylation and stability of *Neurospora* circadian clock protein FRQ. *J. Biol. Chem.* **285**, 11508–11515
27. Gorl, M., Merrow, M., Huttner, B., Johnson, J., Roenneberg, T., and Brunner, M. (2001) A PEST-like element in FREQUENCY determines the length of the circadian period in *Neurospora crassa*. *EMBO J.* **20**, 7074–7084
28. Wang, B., Stevenson, E.-L., and Dunlap, J. C. (2022) Functional analysis of 110 phosphorylation sites on the circadian clock protein FRQ identifies clusters determining period length and temperature compensation. *G3 (Bethesda)* **13**, jkac334
29. Tang, C.-T., Li, S., Long, C., Cha, J., Huang, G., Li, L., *et al.* (2009) Setting the pace of the *Neurospora* circadian clock by multiple independent FRQ phosphorylation events. *Proc. Natl. Acad. Sci. U. S. A.* **106**, 10722–10727
30. Liu, Y., Loros, J., and Dunlap, J. C. (2000) Phosphorylation of the *Neurospora* clock protein FREQUENCY determines its degradation rate and strongly influences the period length of the circadian clock. *Proc. Natl. Acad. Sci. U. S. A.* **97**, 234–239
31. Cha, J., Chang, S.-S., Huang, G., Cheng, P., and Liu, Y. (2008) Control of WHITE COLLAR localization by phosphorylation is a critical step in the circadian negative feedback process. *EMBO J.* **27**, 3246–3255
32. Garceau, N. Y., Liu, Y., Loros, J. J., and Dunlap, J. C. (1997) Alternative Initiation of translation and time-specific phosphorylation yield multiple forms of the essential clock protein FREQUENCY. *Cell* **89**, 469–476
33. Hurley, J. M., Larrondo, L. F., Loros, J. J., and Dunlap, J. C. (2013) Conserved RNA helicase FRH acts Nonenzymatically to support the intrinsically disordered *Neurospora* clock protein FRQ. *Mol. Cell* **52**, 832–843
34. Hurley, J. M., Dasgupta, A., Emerson, J. M., Zhou, X., Ringelberg, C. S., Knabe, N., *et al.* (2014) Analysis of clock-regulated genes in *Neurospora* reveals widespread posttranscriptional control of metabolic potential. *Proc. Natl. Acad. Sci. U. S. A.* **111**, 16995–17002
35. Cheng, P., Yang, Y., and Liu, Y. (2001) Interlocked feedback loops contribute to the robustness of the *Neurospora* circadian clock. *Proc. Natl. Acad. Sci. U. S. A.* **98**, 7408–7413
36. Shi, Mi. (2008) *Circadian and non-circadian oscillators in* Neurospora crassa. Ph.D. thesis, Dartmouth College
37. Liu, X., Chen, A., Caicedo-Casso, A., Cui, G., Du, M., He, Q., *et al.* (2019) FRQ-CK1 interaction determines the period of circadian rhythms in *Neurospora*. *Nat. Commun.* **10**, 4352
38. Hu, Y., Liu, X., Lu, Q., Yang, Y., He, Q., Liu, Y., *et al.* (2021) FRQ-CK1 interaction underlies temperature compensation of the *Neurospora* circadian clock. *mBio* **12**, e0142521
39. Diernfellner, A. C. R., Querfurth, C., Salazar, C., Höfer, T., and Brunner, M. (2009) Phosphorylation modulates rapid nucleocytoplasmic shuttling and cytoplasmic accumulation of *Neurospora* clock protein FRQ on a circadian time scale. *Genes Dev.* **23**, 2192–2200
40. Schafmeier, T., Diernfellner, A., Schäfer, A., Dintsis, O., Neiss, A., and Brunner, M. (2008) Circadian activity and abundance rhythms of the *Neurospora* clock transcription factor WCC associated with rapid nucleo–cytoplasmic shuttling. *Genes Dev.* **22**, 3397–3402
41. Gooch, V. D., Mehra, A., Larrondo, L. F., Fox, J., Touroutoutoudis, M., Loros, J. J., *et al.* (2008) Fully codon-optimized *luciferase* uncovers novel temperature characteristics of the *Neurospora* clock. *Eukaryot. Cell* **7**, 28–37
42. Merrow, M. W., Garceau, N. Y., and Dunlap, J. C. (1997) Dissection of a circadian oscillation into discrete domains. *Proc. Natl. Acad. Sci. U. S. A.* **94**, 3877–3882
43. Cha, J., Yuan, H., and Liu, Y. (2011) Regulation of the activity and cellular localization of the circadian clock protein FRQ. *J. Biol. Chem.* **286**, 11469–11478
44. Diernfellner, A. C. R., Lauinger, L., Shostak, A., and Brunner, M. (2019) A pathway linking translation stress to checkpoint kinase 2 signaling in *Neurospora crassa*. *Proc. Natl. Acad. Sci. U. S. A.* **116**, 17271–17279
45. Diernfellner, A. C. R., and Brunner, M. (2020) Phosphorylation timers in the *Neurospora crassa* circadian clock. *J. Mol. Biol.* **432**, 3449–3465

46. Mehra, A., Shi, M., Baker, C. L., Colot, H. V., Loros, J. J., and Dunlap, J. C. (2009) A role for casein kinase 2 in the mechanism underlying circadian temperature compensation. *Cell* **137**, 749–760
47. Pregueiro, A. M., Liu, Q., Baker, C. L., Dunlap, J. C., and Loros, J. J. (2006) The *Neurospora* checkpoint kinase 2: a regulatory link between the circadian and cell cycles. *Science* **313**, 644–649
48. Wang, B., Zhou, X., Gerber, S. A., Loros, J. J., and Dunlap, J. C. (2021) Cellular calcium levels influenced by NCA-2 impact circadian period determination in *Neurospora*. *mBio* **12**, e0149321
49. Yang, Y., Cheng, P., and Liu, Y. (2002) Regulation of the *Neurospora* circadian clock by casein kinase II. *Genes Dev.* **16**, 994–1006
50. Yang, Y., Cheng, P., Zhi, G., and Liu, Y. (2001) Identification of a calcium/calmodulin-dependent protein kinase that Phosphorylates the *Neurospora* circadian clock protein FREQUENCY. *J. Biol. Chem.* **276**, 41064–41072
51. Larrondo, L. F., Olivares-Yañez, C., Baker, C. L., Loros, J. J., and Dunlap, J. C. (2015) Decoupling circadian clock protein turnover from circadian period determination. *Science* **347**, 1257277
52. Colot, H. V., Park, G., Turner, G. E., Ringelberg, C., Crew, C. M., Litvinkova, L., *et al.* (2006) A high-throughput gene knockout procedure for *Neurospora* reveals functions for multiple transcription factors. *Proc. Natl. Acad. Sci. U. S. A.* **103**, 10352–10357
53. Belden, W. J., Larrondo, L. F., Froehlich, A. C., Shi, M., Chen, C.-H., Loros, J. J., *et al.* (2007) The *band* mutation in *Neurospora crassa* is a dominant allele of *ras-1* implicating RAS signaling in circadian output. *Genes Dev.* **21**, 1494–1505
54. Vogel, H. J. (1956) A convenient growth medium for *Neurospora crassa* (medium N). *Microb. Genet. Bull.* **13**, 42–47
55. Westergaard, M., and Mitchell, H. K. (1947) *Neurospora* V. A synthetic medium favoring sexual reproduction. *Am. J. Bot.* **34**, 573–577
56. Wang, B., Kettenbach, A. N., Gerber, S. A., Loros, J. J., and Dunlap, J. C. (2014) *Neurospora* WC-1 recruits SWI/SNF to remodel *frequency* and initiate a circadian cycle. *PLoS Genet.* **10**, e1004599
57. Wang, B., Zhou, X., Kettenbach, A. N., Mitchell, H. D., Markillie, L. M., Loros, J. J., *et al.* (2023) A crucial role for dynamic expression of components encoding the negative arm of the circadian clock. *Nat. Commun.* **14**, 3371
58. Denault, D. L., Loros, J. J., and Dunlap, J. C. (2001) WC-2 mediates WC-1-FRQ interaction within the PAS protein-linked circadian feedback loop of *Neurospora*. *EMBO J.* **20**, 109–117
59. Larrondo, L. F., Loros, J. J., and Dunlap, J. C. (2012) High-resolution spatiotemporal analysis of gene expression in real time: in vivo analysis of circadian rhythms in *Neurospora crassa* using a FREQUENCY-luciferase translational reporter. *Fungal Genet. Biol.* **49**, 681–683
60. Zhou, X., Wang, B., Emerson, J. M., Ringelberg, C. S., Gerber, S. A., Loros, J. J., *et al.* (2018) A HAD family phosphatase CSP-6 regulates the circadian output pathway in *Neurospora crassa*. *PLoS Genet.* **14**, e1007192